BOREAL ENVIRONMENT RESEARCH 14: 591–605
ISSN 1239-6095 (print) ISSN 1797-2469 (online)

Helsinki 31 August 2009

Long-term field measurements of charged and neutral clusters using Neutral cluster and Air Ion Spectrometer (NAIS)

Hanna E. Manninen[1)], Tuukka Petäjä[1)], Eija Asmi[1),3)], Ilona Riipinen[1)], Tuomo Nieminen[1)], Jyri Mikkilä[1)], Urmas Hõrrak[2)], Aadu Mirme[2)], Sander Mirme[2)], Lauri Laakso[1)], Veli-Matti Kerminen[3)] and Markku Kulmala[1)]

[1)] *Department of Physics, P.O. Box 64, FI-00014 University of Helsinki, Finland*
[2)] *Institute of Physics, Laboratory of Environmental Physics, University of Tartu, Ülikooli 18, EE-50090 Tartu, Estonia*
[3)] *Finnish Meteorological Institute, Research and Development, P.O. Box 503, FI-00101 Helsinki, Finland*

Received 17 Feb. 2009, accepted 5 May 2009 (Editor in charge of this article: Jaana Bäck)

Manninen, H. E., Petäjä, T., Asmi, E., Riipinen, I., Nieminen, T., Mikkilä, J., Hõrrak, U., Mirme, A., Mirme, S., Laakso, L., Kerminen, V.-M. & Kulmala, M. 2009: Long-term field measurements of charged and neutral clusters using Neutral cluster and Air Ion Spectrometer (NAIS). *Boreal Env. Res.* 14: 591–605.

To understand the very first steps of atmospheric particle formation and growth, measurements at the size where atmospheric nucleation occurs are crucially needed. We present number size distributions of > 0.8 nm ions and > 1.8 nm particles measured with the Neutral cluster and Air Ion Spectrometer (NAIS) at a boreal forest site in Hyytiälä, Finland, during 2006–2007. Pools of neutral and charged clusters seem to be present all the time below 3 nm. The total concentration of 1.8–3.0 nm clusters was ~1000 cm^{-3}, ranging from 50 to 6000 cm^{-3}, whereas the concentrations of charged clusters in this size range remained below 50 cm^{-3}. On average, both neutral and charged clusters seem to have different diurnal cycles on particle formation event and non-event days. We also compared the NAIS-derived concentrations with those obtained from other concurrent air ion and particle instruments and found that the NAIS concentrations are in agreement with concentrations determined with these other instruments.

Introduction

Aerosol particles affect the climate and visibility by scattering and absorbing incoming solar radiation and by influencing many cloud properties (Cabada *et al*. 2004, Lohmann and Feichter 2005, Bellouin *et al*. 2008, Hyslop *et al*. 2009). One source for atmospheric aerosol particles is nucleation, a phenomenon observed to frequently take place in various environments in the boundary layer as well as in the free troposphere (Kulmala *et al*. 2004, Kulmala and Kerminen 2008, and references therein). Measurements demonstrate further that aerosol particles nucleated in the atmosphere may reach sizes at which they participate in cloud processes (e.g. O'Dowd *et al*. 1999, Lihavainen *et al*. 2003, Kerminen *et al*. 2005, Laaksonen *et al*. 2005, Kuwata *et al*. 2008). Atmospheric model investigations suggest that atmospheric nucleation can be con-

sidered a globally important source of aerosol particles and cloud condensation nuclei (Adams and Seinfeld 2002, Spracklen *et al*. 2008, Yu *et al*. 2008, Pierce and Adams 2009, Makkonen *et al*. 2009, Wang and Penner 2009). In spite of the potential importance of atmospheric nucleation, several unresolved questions about this phenomenon still exist. One of the most important reasons for this has been the lack of direct atmospheric measurements at the size where the initial steps of the atmospheric nucleation take place (Kulmala *et al*. 2007a).

Several formation mechanisms for atmospheric aerosol particles have been suggested. These include activation of stable neutral clusters (Kulmala *et al*. 2000, 2006, Eisele *et al*. 2005, Sihto *et al*. 2006), activation of sulfur radicals (Berndt *et al*. 2008, Laaksonen *et al*. 2008), kinetic nucleation (Weber *et al*. 1996), ion-induced (Laakso *et al*. 2002, Lovejoy *et al*. 2004) and ion-mediated nucleation (Yu and Turco 2000), as well as binary and ternary homogeneous nucleation (Vehkamäki *et al*. 2002). The existence of neutral clusters is suggested by theoretical arguments (Kulmala *et al*. 2005), laboratory (Hanson and Eisele 2002) and field experiments (Kulmala *et al*. 2007a, Lehtipalo *et al*. 2008, Sipilä *et al*. 2008). The role of ion-induced nucleation in new particle formation is still under discussion (Iida *et al*. 2006, Laakso *et al*. 2007, Kulmala *et al*. 2007a, Kazil *et al*. 2008, Yu *et al*. 2008). Although sulfuric acid is connected to the atmospheric particle formation (Weber *et al*. 1997, Riipinen *et al*. 2006, Sihto *et al*. 2006, Kuang *et al*. 2008), recent studies (Hirsikko *et al*. 2005, Ehn *et al*. 2005, Riipinen *et al*. 2009) suggest that also organics take part in the subsequent particle growth.

Finding out the relative importance of different aerosol formation mechanisms and quantifying their role in atmospheric cloud condensation nuclei production requires better understanding on the behavior of nanometer-size clusters in the atmosphere. The lower detection limit of the majority of the commercially available aerosol instruments is 3 nm (McMurry 2000a), while atmospheric nucleation and cluster activation is expected to take place at particle sizes of 1.5–2 nm (Kulmala *et al*. 2007a) in diameter. Atmospheric charged clusters even smaller than 1 nm can be detected with ion spectrometers (Tammet *et al*. 2006, Mirme *et al*. 2007). Natural charge of the ions enables the electrical detection (Flagan 1998), given that the concentrations are large enough. The sub-3 nm neutral particles are challenging to classify and detect in many respects and the recent instrumental development has pushed the neutral particle detection limit below 2 nm in size (e.g. Sipilä *et al*. 2008, Sipilä *et al*. 2009, Iida *et al*. 2009) with various condensation/activation techniques. In the case of condensation techniques the activation efficiency determines smallest detectable particle size (Stolzenburg and McMurry 1991, Kulmala *et al*. 2007b, Winkler *et al*. 2008).

The electrical detection of the clusters is a challenging task due to small concentrations, transport losses and insufficient charging efficiency of the small neutral particles. Thus, the electrical instruments need to be sensitive enough to distinguish the minuscule signal brought in by the clusters from the instrument background. To tackle the difficulties in the electrical techniques, sample flow rate can be increased, which leads to higher currents both due to higher absolute concentration carried by the ions to the detector per a given unit of time as well as due to reduced losses of the ions during the transport. By utilizing a unipolar charger, the charging efficiency can be improved.

We measured mobility distributions of 0.8–47 nm neutral and charged aerosol particles and clusters continuously with a Neutral cluster and Air Ion Spectrometer (NAIS) in a boreal forest region during 2006–2007. Kulmala *et al*. (2007a) reported on the first atmospheric cluster measurement using NAIS to evaluate the concentrations and dynamics of atmospheric clusters. Asmi *et al*. (2009) tested the operation of the NAIS in laboratory calibrations. In this paper we present the first long-term NAIS field measurement data. The sensitivity of the NAIS will be studied in comparison with other aerosol instrumentation. In addition, we will investigate how the concentrations and size distribution of total and charged clusters behave in the long term at sizes where the real atmospheric nucleation and activation occurs. This is crucial to our understanding of the very first steps of new particle formation events in the atmosphere. Within

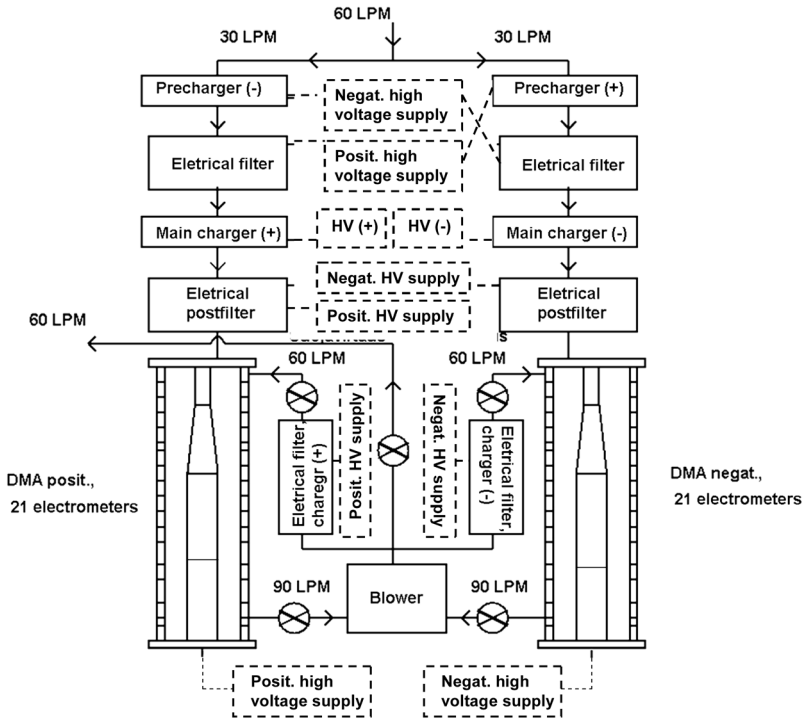

Fig. 1. A schematic picture of the Neutral Cluster and Air Ion Spectrometer (NAIS).

the EUCAARI project (Kulmala *et al*. 2009), several NAIS instruments are being used in continuous field measurements around the Europe. Therefore, this study provides a significant value when interpreting EUCAARI cluster spectrometer data.

Material and methods

We performed field measurements at the SMEAR II (Station for Measuring Forest Ecosystem–Atmosphere Relations II) station located at Hyytiälä, southern Finland (61°51´N, 24°17´E, 181 m a.s.l.; for more details *see* Hari and Kulmala 2005). The station is equipped with extensive facilities to measure continuously and comprehensively forest ecosystem–atmosphere interactions (Kulmala *et al*. 2001). Boreal, homogeneous Scots pine forest surrounds the station. This study focuses purely on aerosol concentration and size distribution measurements within the forest canopy. The data considered here were collected during 48 weeks in the years 2006 and 2007. The mobility distribution of neutral particles and ions was measured with the Neutral cluster and Air Ion Spectrometer (NAIS, Airel Ltd., Estonia). The ion mobility distribution was measured with two different ion spectrometers (Airel Ltd., Estonia): Balanced Scanning Mobility Analyzer (BSMA, Tammet 2006) and Air Ion Spectrometer (AIS, Mirme *et al*. 2007). The aerosol particle number size distribution was measured with a Differential Mobility Particle Sizer (DMPS, Aalto *et al*. 2001). The total particle concentrations were measured with Condensation Particle Counters (CPCs, TSI Inc., USA, McMurry 2000b).

Neutral cluster and Air Ion Spectrometer (NAIS)

The NAIS is an instrument capable of measuring mobility distributions of sub-3 nm neutral and charged aerosol particles and clusters (Fig. 1). The NAIS was developed from the Air Ion Spectrometer (AIS, Mirme *et al*. 2007) by Airel Ltd., Estonia. Controlled charging, together with the electrostatic filtering, enables it to distinguish the neutral aerosol particles from the naturally charged ions. The measurement principle of the

NAIS is based on unipolar charging of the sampled particles and their subsequent detection with an electrical mobility analyzer. The mobility range of the NAIS is 3.16–0.001 $cm^2\ V^{-1}\ s^{-1}$, which corresponds to a mobility diameter range of 0.8–47 nm (Millikan-Fuchs equivalent diameter, Mäkelä *et al*. 1996). The NAIS measures ion and particle number distribution in 21 size fractions with a five-minute time resolution to optimize sensitivity and signal-to-noise ratio.

The NAIS consists of two independent spectrometer columns, one of each polarity, where the ions are classified by a cylindrical differential mobility analyzer (DMA). The inner cylinder of the analyzer is geometrically divided into four insulated, ion-repulsive sections. The ion-collecting, outer cylinder has 21 electrically-isolated electrometer rings. The radial electrical field is generated by connecting a potential to all four sections of the inner cylinder. The ions are simultaneously classified and collected to the electrometer rings in the outer cylinder according to their electrical mobilities, and the ion currents are measured with the electrometers. The sample and sheath flows of the analyzers are 30 and 60 l min^{-1}, respectively. The ratio of sample and sheath flows is 1:2, widening the measurement channel transfer functions (Knutson and Whitby 1975) and spreading the detection of monomobile ions to several channels (Asmi *et al*. 2009). The high flow rates are used to minimize the ion diffusion losses and also increase the sensitivity to the ion concentrations. The flows are checked with venturi flow tubes and adjusted in flow calibrations (Asmi *et al*. 2009). Both of the mobility analyzers have a closed loop sheath flow arrangements.

The NAIS has two unipolar corona-wire diffusion charger (Biskos *et al*. 2005) and electrostatic post-filter pairs prior to the mobility analyzers in both polarities (Fig. 1). One pair is for positive and one for negative charging. The post-filters are used to remove the ions generated by the chargers. The particle charging probabilities are predicted by Fuchs' diffusion charging theory (Fuchs and Sutugin 1971). Kulmala *et al*. (2007a and supporting material therein) presented the particle charging probability in the NAIS. At a constant corona-wire current the aerosol charging depends mainly on the particle size, concentration and the residence time of the aerosol in the charging region. The sampled particles are assumed to be in charge equilibrium. The lower detection limit of the NAIS is determined by the charging probabilities, cluster concentration and the mass and mobility of charger ions. Asmi *et al*. (2009) reported that under NTP (temperature = 293.15 K, pressure = 101.325 hPa) conditions, the negative corona ions ranged from 0.9 to 1.5 nm in mobility diameter, whereas the positive corona ions ranged from 1.0 to 1.8 nm. Therefore, the lowest estimate for the detection limit is approximately 1.8 nm. Particles below these limits cannot be reliably distinguished from the charger ions. The production and parameters of corona ions can change depending on environmental conditions.

The NAIS measures in ion, particle and offset modes to define the ion and the particle spectrum. In the ion mode, both pairs of corona chargers and electrostatic filters are switched off. Therefore, the instrument classifies and detects ions according to their ambient charge. In the particle mode, the latter pair of the corona chargers and the post-filters is switched on. The charger polarity is equal to the analyzer polarity. Therefore, all the particles carried into the DMA are either uncharged or charged with the same polarity as the analyzer. In the offset mode, the foremost pair of the unipolar corona chargers, which has the opposite polarity to the analyzers, and the electrostatic filters are switched on. The opposite charging together with the filtration enables us to measure the noise and the offset of the electrometers, when no particles or ions are carried to the DMA. A similar filtration is used also for cleaning the re-circulated sheath air. After each ion- and particle-mode spectrum, offset of the electrometers is measured and subtracted from the measured electrometer signal. The NAIS has an additional operation mode, called alternate charging, to bring particles closer to an equilibrium charge distribution. Prior the charging, the sampled particles are exposed to the corona ions of an opposite sign.

Supplementary instrumentation

The Balanced Scanning Mobility Analyzer

(BSMA, Tammet 2006) measures mobility distributions of charged clusters and nanoparticles of both negative and positive polarity. The mobility range of the BSMA is from 3.2 to 0.032 $cm^2\ V^{-1}\ s^{-1}$, which corresponds to a mobility diameter range of 0.8 to 8.0 nm. The BSMA consists of two plane-type differential mobility analyzers, one for each polarity, and a common electrical amplifier connected to a balanced bridge circuit. Inside each analyzer there is a collecting element connected to a common electrometer for measuring the electrical current of air ions. The scanning of the mobility distribution is carried out by discharging a capacitor through the repelling electrode and monitoring the electrometer current with the balanced bridge circuit. The BSMA measures number distribution in 16 size fractions with a 10-minute time resolution.

The Air Ion Spectrometer (AIS, Mirme *et al*. 2007) measures mobility distributions of both negative and positive air ions in the range from 3.16 to 0.0010 $cm^2\ V^{-1}\ s^{-1}$. This corresponds to a mobility diameter range of approximately 0.8 nm to 47 nm. The AIS consists of two cylindrical-type differential mobility analyzers, one of each polarity, with 21 insulated electrometer rings on outer cylinder. The inner electrode of the cylindrical DMA is geometrically designed and connected to four different high voltages. Therefore, the electrometer rings measure simultaneously all electrical mobility fractions for both polarities. As compared with the NAIS, the AIS lacks the additional pair of corona chargers and electrostatic filters needed for the unipolar charging of the sampled particles with the total particle mode measurements. The AIS measures with a five-minute time resolution.

The Differential Mobility Particle Sizer (DMPS) setup measures atmospheric aerosol particle number size distribution between 3 and 1000 nm in diameter. The setup consists of two parallel DMPS units, which have different but partly overlapping measuring ranges. Both units use a Hauke-type DMA (lengths 28.0 cm or 10.9 cm), CPC (TSI 3025 or 3010) as a particle detector, closed loop sheath flow arrangements (Jokinen and Mäkelä 1996) and the same radioactive Krypton-85 beta neutralizer. The complete size distribution is obtained with a 10-minute time resolution by changing the classifying voltage of the DMA. The setup is described in more detail in Aalto *et al*. (2001). Total aerosol number concentration is calculated from the measured number size distribution.

The particle charging state is measured with an Ion-DMPS (Laakso *et al*. 2007). The instrument measures continuously the concentrations of ions in ambient and charge equilibrated air in the diameter range of 3–15 nm (6 March to 15 December 2006) and 2–11.5 nm (16 December 2006 to 27 August 2007). The Ion-DMPS consists of a Hauke-type DMA (short one, 10.9 cm), a CPC (TSI 3025) and a Nickel-63 beta neutralizer. The switching of DMA's polarity between negative and positive potential and the switching on and off the neutralizer enables to measure the natural charging state of the particles (concentration measured without the charger divided by the corresponding charged particle concentration). The Ion-DMPS measures number distribution of ions in seven size fractions with a 13-minute time resolution.

Results and discussion

We began mobility distribution measurements of the neutral and charged particles and clusters with the NAIS in Hyytiälä in March 2006. The data used in this study were collected during the following three periods: 6 March to 16 May 2006, 14 September to 15 December 2006, and 8 March to 27 August 2007. We had a total of 48 weeks of data. We calculated various median characteristics based on the NAIS data to obtain long-term information about the diurnal and seasonal variations of particle and cluster concentrations and size distributions. The sensitivity of the NAIS data was investigated in comparison to other concurrent air ion and aerosol particle instrumentation.

General features

Typical data measured with the NAIS on a particle formation event days are presented for the period 8–19 April 2007 (Fig. 2). The period consists of 12 consecutive days with clear new particle formation (NPF) and growth in the smallest

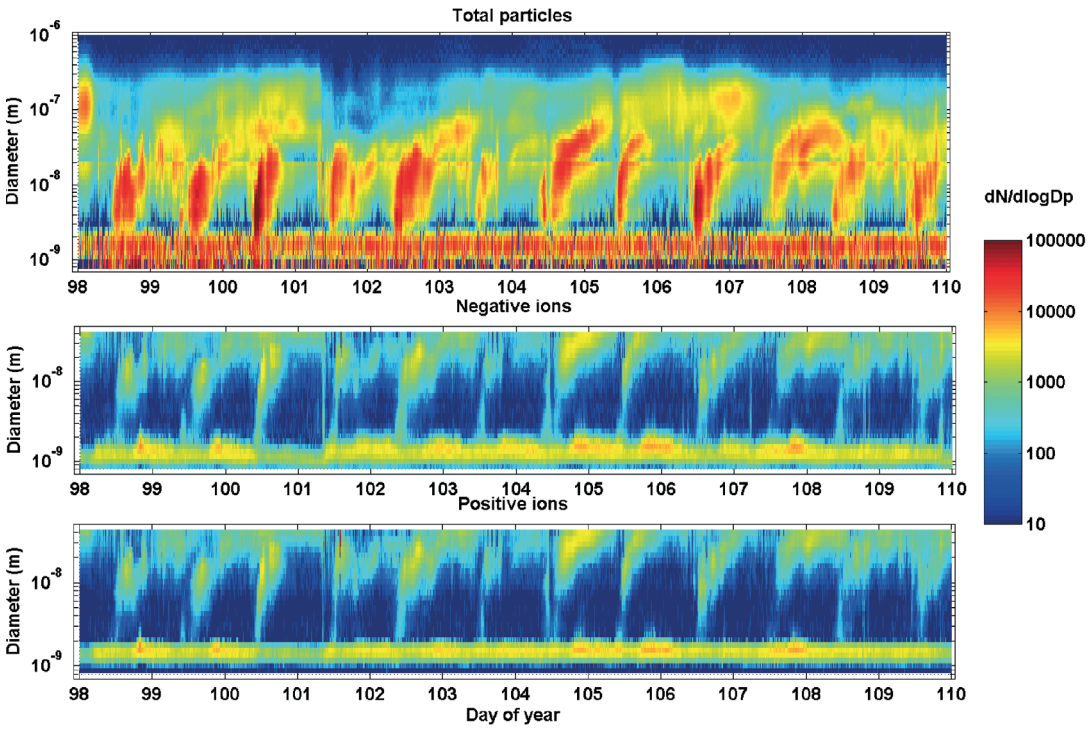

Fig. 2. Total particle size distribution measured with the NAIS positive charging mode in the size range 0.8–20 nm and with the DMPS in the size range 20–1000 nm (top). Negative (middle) and positive (bottom) air-ion distributions were measured with the NAIS ion mode (0.8–40 nm) on 12 consecutive particle formation event days between 8 and 19 April 2007 in Hyytiälä, Finland.

size range. On all the days, the distinct shape of the formation and growth (Dal Maso *et al*. 2005) was observed. Typically the formation of sub-3 nm particles began around noon and the growth of the particles continued several hours towards the Aitken mode. In other words, clusters activated in the morning and started growing by condensation.

The time series of negative and positive ion size distributions were similar to that of the neutral cluster size distribution. The observed formation and growth of particles and ions seemed to be almost simultaneous during NPF events. Nevertheless, on some days that had been classified as NPF event days (Dal Maso *et al*. 2005), the charged cluster concentrations were seen to increase somewhat before the corresponding increase in total cluster concentrations. The term 'total cluster' refers to the sum of charged and neutral clusters. During the measurements, 100 particle formation event days were observed. No new particle formation was observed on 91 days, and 145 days could not be reliably classified as either an event or non-event day. On days with no indication of particle formation, throughout the whole day charged and neutral cluster size distributions were typically similar to those at nighttime seen Fig. 2.

Pools of charged and neutral clusters seemed to be continuously present at sizes below 3 nm (Figs. 2 and 3). According to our measurements, the pool of charged clusters had a median size of ~1.1–1.3 nm, being slightly smaller in negative polarity. The pool of neutral clusters was extending from ~1–2.6 nm in size with a median of ~1.7 nm. The smallest clusters (< 1.8 nm) detected in the neutral cluster pool were originating from the corona charger (Asmi *et al*. 2009). The existence of atmospheric ion clusters has been known for decades (Kulmala and Tammet 2007), whereas the existence of neutral clusters has not been measured until recently with newly-developed measurement techniques. Kulmala *et al*. (2007) reported the first observations of the pool of

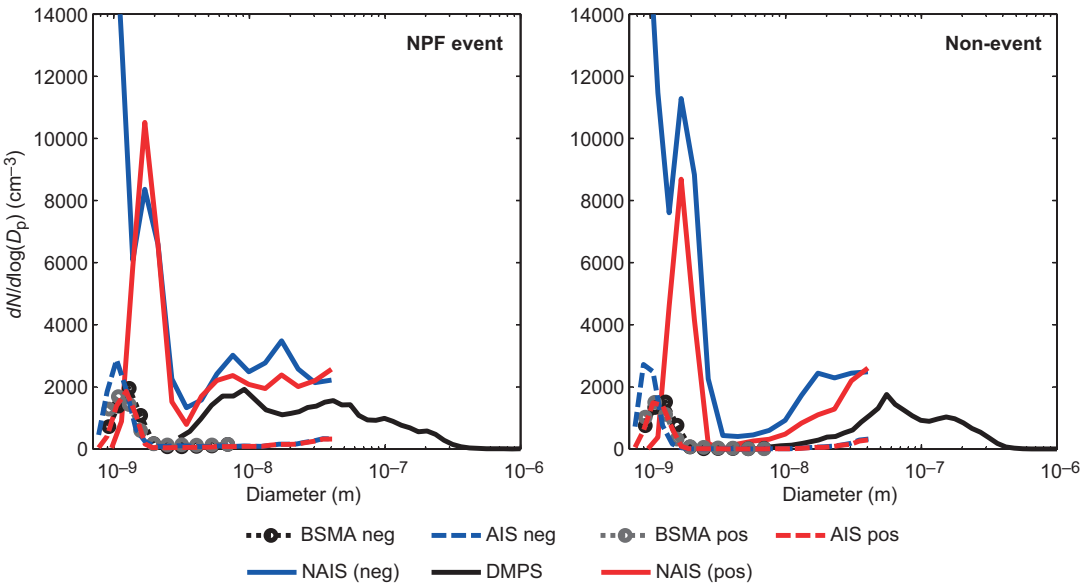

Fig. 3. Two-hour (12:00–14:00) median particle and ion number size distributions measured with the NAIS (with negative and positive charging), DMPS, AIS and BSMA during particle formation event (left-hand-side panel) and non-event (right-hand-side panel) days in spring 2006.

neutral clusters in the sub-3 nm range based on the NAIS measurements. Sipilä *et al*. (2008, 2009) and Lehtipalo *et al*. (2008) reported that the sub-3 nm cluster concentrations in Hyytiälä varied from some thousands to 100 000 cm^{-3}, as measured by the pulse-height analyser (Marti *et al*. 1996, Sipilä *et al*. 2008). The observations by Sipilä *et al*. (2008) and Lehtipalo *et al*. (2008) supported the idea of a continuously present pool of numerous clusters in the sub-3 nm size range.

Cluster number size distributions

Cluster number size distributions were measured with several instruments (Fig. 3). In the overlapping size range, a good agreement in the distributions of charged clusters between the AIS and the BSMA was usually observed. The median size of the negative cluster pool was smaller than that of the positive one, and they both were smaller than the median size of the total cluster pool. In the size range close to the molecular scale, the chemical composition of the clusters determines their charging efficiency. Also the concentration of cluster pool depended on the polarity. In the 3–40 nm size range, the NAIS detected more particles as compared with the DMPS and the agreement was only qualitative.

The difference between the NAIS and DMPS readings originates from data inversion assumptions. In the number size distribution data inversion, we should assume some kind of particle size distribution outside the measurement range. With the DMPS, this is solved by using PM-1 impactor in front of the sample inlet (cut-off 1 μm). Therefore, we know that the sample air of the DMPS system does not include particles outside the upper measurement range. With the NAIS it is not possible to use an impactor due to high sample flow rate as limitations in available impactors with a correct cut-off size, and this would add the sampling losses of the smaller particles and ions. Thus, the NAIS measurements are affected by the changing size distribution of particles outside the instrument's upper measurement range. All the particles entering the NAIS are assumed to be in charge equilibrium. Only singly-charged particles are taken into account in the NAIS data inversion. The NAIS is in a better agreement with the lower end of the DMPS (< 20 nm) in the overlapping size range, where the effects of the multiple charging become negligible (Fig. 2, top panel).

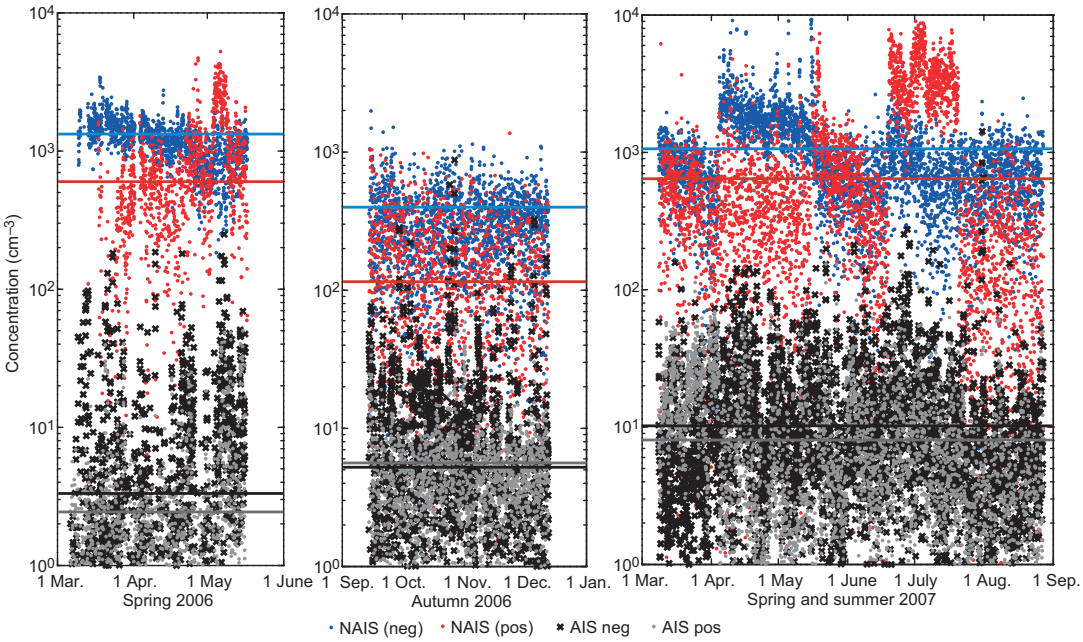

Fig. 4. Concentrations of 1.8–3 nm negative and positive ions measured with the AIS (black crosses and gray dots) and particles with negative and positive charging of the sample measured with the NAIS (blue and red dots) during 48 weeks of measurement. Lines indicate the median concentrations during a particular season. The ion concentration was measured with the AIS on 6 March to 16 May 2006 and with the NAIS (in AIS-mode) on 14 September to 15 December 2007 and on 3 March to 27 August 2008.

The negative and positive charging of the sample in the NAIS yields somewhat different cluster distributions. The differences between the polarities in the lowest channels of the NAIS result from the operation of the post-filters and corona chargers. The post-filters are designed to remove all ions produced by the corona chargers. In the present design of the instrument, the post-filter's operating voltage is adjusted by the user. The calibration of the post-filters and the correct adjusting is challenging due to reference instrument limitations. In an ideal case, all the corona ions are removed but still the detection limit is kept as low as possible for the sampled clusters. In a worst case scenario all of the sampled clusters are filtered. The filtering removes always some part of the sampled clusters. The size range of the charger ions sets the lower detection limit of the NAIS to ~1.8 nm depending on polarity and cluster concentrations. Asmi *et al*. (2009) reported that in indoor measurements under NTP conditions the negative and the positive corona ions were < 1.5 nm and < 1.8 nm, respectively. As mentioned before, even clusters having a single distinct mobility are detected by the NAIS in approximately 3–5 electrometer channels (Asmi *et al*. 2009). Therefore, the effect of the corona charger could be seen at sizes larger than 1.8 nm.

Cluster concentrations

According to the NAIS data (Fig. 4) obtained by negative charging of the sample, the concentration of 1.8–3.0 nm total clusters was of the order of 1000 cm^{-3} ranging from about 50 to 6000 cm^{-3}. The median concentrations for clusters in size range of 1.8–3.0 nm were 1290 cm^{-3} in spring 2006, 390 cm^{-3} in autumn 2006 and 1010 cm^{-3} in spring and summer 2007. On average, the total cluster concentrations during the spring time were higher than during the autumn. Lehtipalo *et al*. (2008) reported that in Hyytiälä, the median concentration of ~1.5–3 nm clusters in spring 2007 was about 8000 cm^{-3}, varying from 500 to 50 000 cm^{-3}. Therefore, the size range of ~1.5–1.8 nm is expected to contain

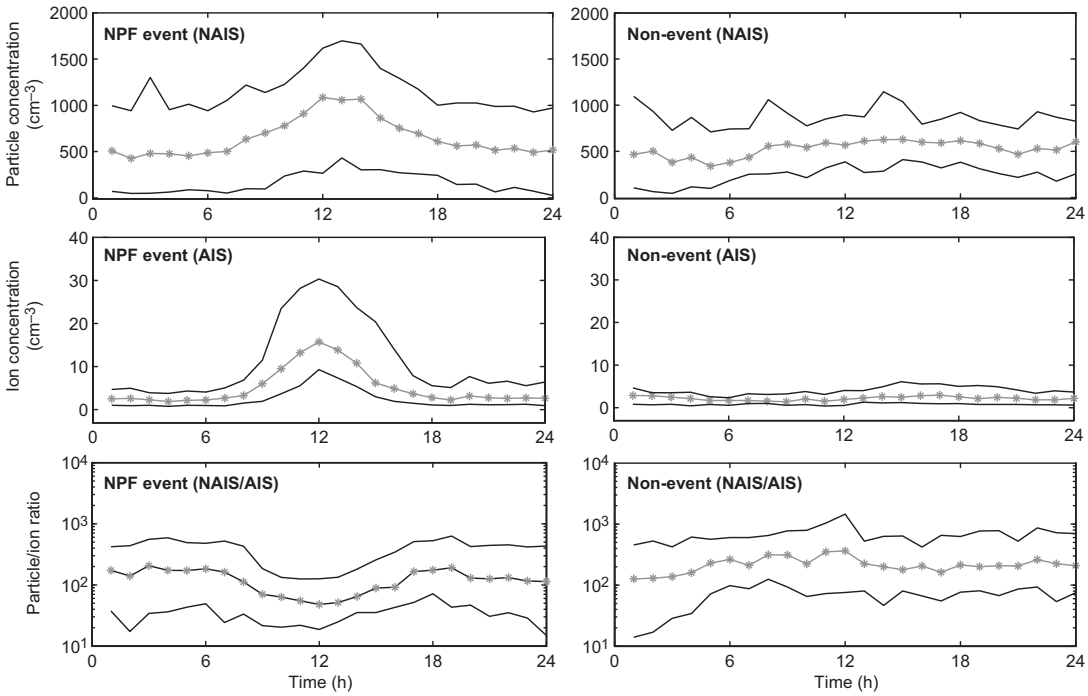

Fig. 5. The median diurnal cycle of 1.8–3 nm particle and air ion concentrations measured with the positive polarity of the NAIS and the AIS, respectively, and median diurnal ratio of these two concentrations (gray lines with crosses) on the NPF event and non-event days between 6 March and 15 June 2006 in Hyytiälä. Black solid lines are the corresponding 25 and 75 percentiles.

a large number of neutral clusters. By measuring total clusters with the negative charging of the sample, we detected typically higher cluster concentrations compared to the positive charging. The difference between the cluster concentration readings with the negative and the positive charging can originate from the charging procedure, i.e. production of the corona charger ions and charging probabilities. The manual adjustment of the post-filter operating voltage changes the cut-off size of the instrument. Therefore, the post-filter adjustment is typically seen in the cluster concentrations as a sudden change in concentration level (Fig. 4). Improved, updated versions of the NAIS include automatic adjustment of the post-filters. The apparent trends in cluster concentration in Fig. 4 are caused by the instrument drift.

The concentrations of charged clusters in the size range of 1.8–3.0 nm remained below 50 cm^{-3} (Fig. 4). Ions in the 1.8–3.0 nm size range existed typically during the NPF events. On average, the charged cluster concentrations were higher during the spring time than during the autumn. The ion concentration was measured with the AIS on 6 March to 16 May 2006 and with the NAIS on 14 September to 15 December 2007 and 3–27 August 2008. The ion concentrations measured with the AIS were higher as compared with the ones measured with the NAIS. The difference in concentration readings between the ion spectrometers will be discussed later in this paper. The concentration of < 3 nm total clusters was much higher than the concentration of < 3 nm charged cluster due to low charging probability of the particles at these sizes.

The diurnal variation of the 1.8–3.0 nm particle and ion concentrations differed between particle formation event and non-event days (Fig. 5). During NPF events, both negative and positive median ion concentrations as well as total cluster concentrations were clearly higher than during non-event days. Since the size range of 1.8–3.0 nm is over the cluster ion mode (diameter < 1.6 nm), almost no ions were present in

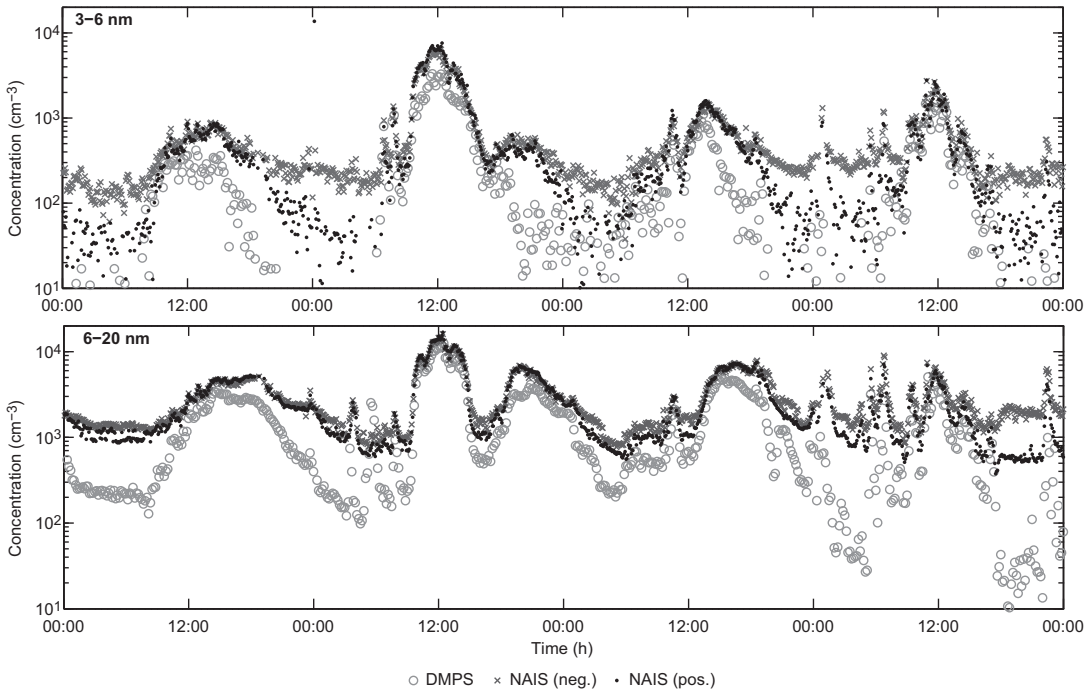

Fig. 6. Total concentrations of particles in the size range 3–6 nm (top panel) and 6–20 nm (bottom panel) measured with the NAIS and the DMPS on 22–25 April 2006 in Hyytiälä.

the air when no nucleation occurred. On the days with indications of new particle formation and growth, an increase in the median concentration of 1.8–3.0 nm total clusters was typically detected around noon, reaching a maximum at midday. The positive polarity was on average more sensitive to the increase in the total cluster concentration. During the first steps of the NPF and growth, the particle to ion ratio decreased, being indicative of a change in the relative fraction of neutral clusters (Fig. 5, bottom left panel). The decrease in neutral cluster fraction at the beginning of nucleation event is connected to the relative importance of ions on new particle formation (Kulmala *et al*. 2007a, 2007b) and on so called overcharging of atmospheric particles (Laakso *et al*. 2007). During overcharging the charged fraction of particles is higher than in charge equilibrium. On 51 days of 100 event days, the decrease of the ratio was observed at the same time as overcharging of the negative ions with the ion-DMPS. The corresponding number for positive overcharging was 34 days out of 100 event days. On the days that had not been classified as the NPF event days, the median total cluster concentration had no clear diurnal cycle.

The particle number concentrations measured with the NAIS were compared with the concentrations measured with the DMPS on example time period 22–25 April 2006 (Fig. 6). The difference between the instruments was lowest during the highest concentrations, whereas at low concentrations the NAIS background concentration corrupted the signal. The positive charging of the sample seemed to agree better with the DMPS data than the negative polarity. The agreement between the NAIS polarities was better in the size range 6–20 nm, indicating that corona charger ions may have effect also in 3–6 nm size range. Lehtipalo *et al*. (2008) compared total cluster concentrations measured by the NAIS and the pulse-height CPC (Sipilä *et al*. 2008). The instruments agreed well in the 3–5 nm size range. The agreement was better for negative charging of the NAIS sample. In the 1.5–3 nm size range the sensitivity of both instruments limited the agreement.

Figure 7 presents the same data as Fig. 6 but in a different way. On these four consecutive NPF

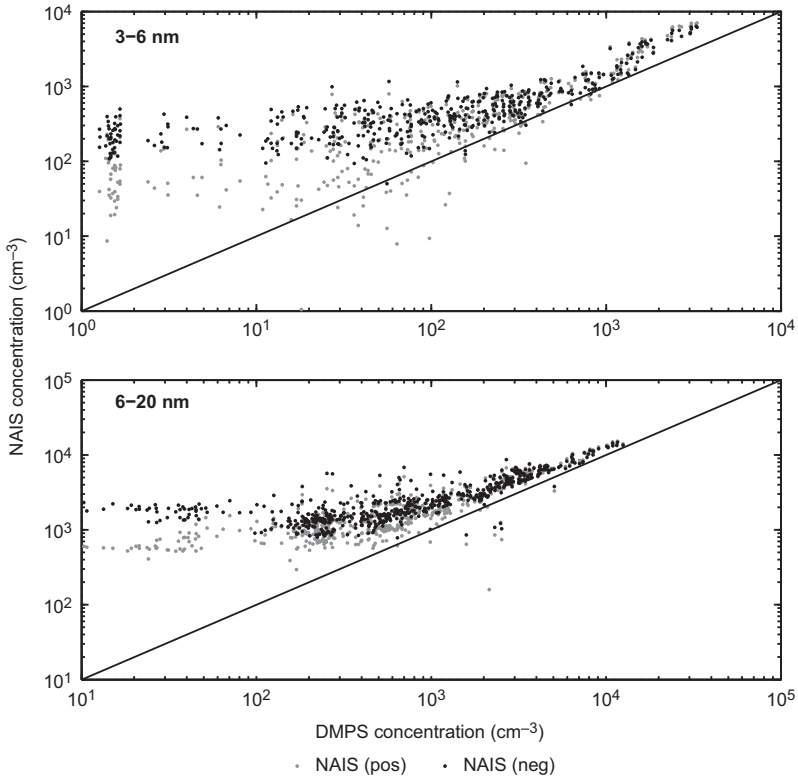

Fig. 7. Total particle concentrations in the size ranges 3–6 nm (top panel) and 6–20 nm (lower panel) measured with the NAIS negative (black dots) and positive (gray dots) charging as a function of corresponding concentration measured with DMPS on 22–25 April 2006 in Hyytiälä.

event days, the concentrations of 3–6 and 6–20 nm particles were never below 100 and 800 cm^{-3}, respectively, indicating a continuous background concentration in the NAIS. The background is partly due to the electrometer noise and partly the processing of negative values in the inversion (Asmi *et al*. 2009). This background is relevant only at the low concentrations. Especially during the NPF events when the particle concentrations typically exceed these values, the NAIS is a capable tool for quantitative measurements. Comparison of the charged cluster concentration in the size range of 1.8–3 nm measured with the NAIS (without charging) with the ones measured with the AIS and the BSMA on 28 April to 1 May 2007 indicates that the concentrations of negative and positive clusters agree remarkably well (Fig. 8). Again, the background of the instruments limited detection at low concentrations. The NAIS detected continues background of ~1–10 ions per cubic centimeter for both polarities in the size range of 1.8–3 nm, being somewhat higher for negative than positive (Fig. 8).

Conclusions

We detected continuously present pools of charged and neutral clusters in the sub-3 nm size range during the 48 weeks of field measurements. Our observations are consistent with other field measurements in Hyytiälä (Kulmala *et al*. 2007a, Lehtipalo *et al*. 2008, Sipilä *et al*., 2008) and support the idea of stable neutral clusters (Kulmala *et al*. 2005). The concentration of 1.8–3.0 nm clusters was ~1000 cm^{-3} ranging from 50 to 6000 cm^{-3}, while the concentrations of charged clusters in this size range remained below 50 cm^{-3}. Negative and positive ions, as well as neutral clusters measured with negative and positive charging, have some difference in the measured number distributions. Typically the median size and the concentration of negative ion clusters were somewhat higher than that of positive ion clusters. The same was true for negative and positive charged samples in detection of the total cluster concentrations.

The total cluster concentrations during the

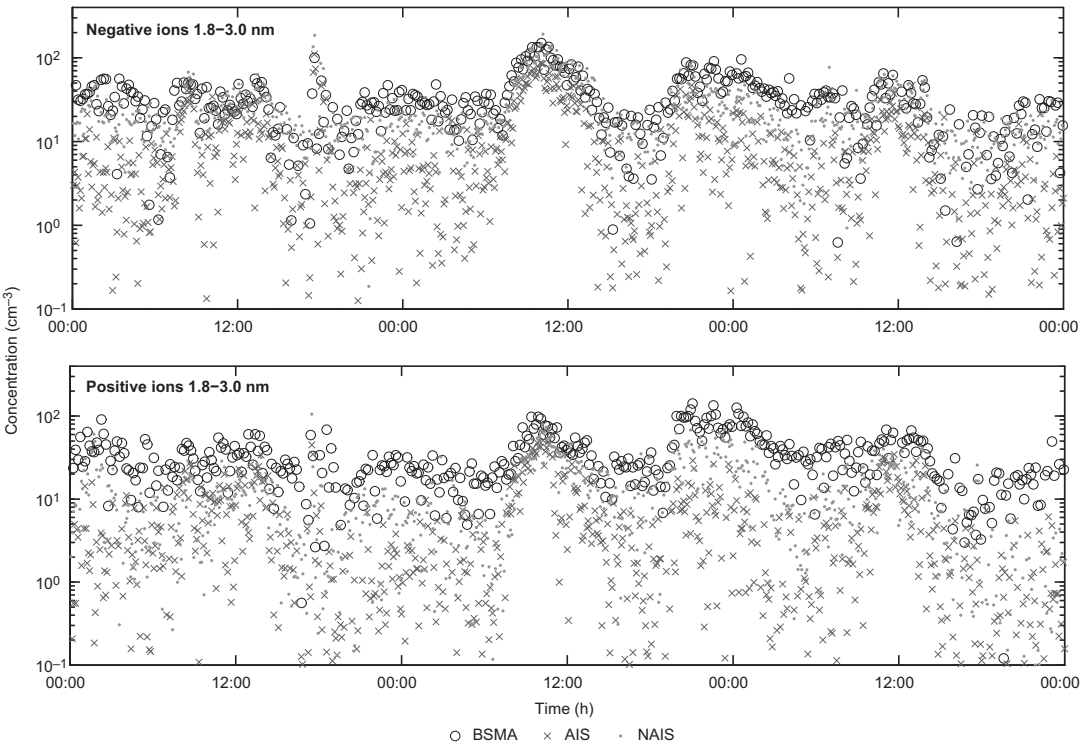

Fig. 8. Number concentrations of the negative (top panel) and positive (bottom panel) charged clusters in the size range 1.8–3.0 nm measured with the NAIS, AIS and BSMA between 28 April and 1 May 2007 in Hyytiälä.

spring were on average higher than during the autumn. The diurnal variation of the 1.8–3.0 nm particle and ion concentrations differed between the particle formation event and non-event days. On the particle formation event days, an increase in the median concentration of 1.8–3.0 nm total and charged clusters was typically detected around noon reaching a maximum at midday.

The performance of NAIS was compared with that of other aerosol and cluster instruments. A quantitative difference between the NAIS and the other aerosol particle instruments originated partly from data inversion assumptions and from the widening of the measurement setup transfer functions. The first steps towards the solution were already made by Asmi *et al*. (2009) by experimentally determining the NAIS transfer functions. The instrument natural background should be also taken into account when converting the instrument signal to the mobility number size spectrum.

Here we have shown that the NAIS is a promising tool to measure size and concentration of atmospheric clusters and particles and can be continuously used under atmospheric conditions. As already presented by Kulmala *et al*. (2007a), the NAIS is able to observe atmospheric new particle formation. In the present study we have shown that during the nucleation events, the total to charged cluster ratio decreased. This observation suggests that relative fraction of ion mediated nucleation is increasing at the beginning of the event. This observation gives good basis for future studies to investigate atmospheric nucleation processes.

Acknowledgements: This work has been partially funded by European Commission 6th Framework program project EUCAARI, contract no. 036833-2 (EUCAARI). The support by the Academy of Finland Centre of Excellence program (project nos. 211483, 211484 and 1118615) is also gratefully acknowledged.

References

Aalto P., Hämeri K., Becker E., Weber R., Salm J., Mäkelä

J.M., Hoell C., O'Dowd C.D., Karlsson H., Hansson H.-C., Väkevä M., Koponen I.K., Buzorius G. & Kulmala M. 2001. Physical characterization of aerosol particles during nucleation events. *Tellus* 53B: 344–358.

Asmi E., Sipilä M., Manninen H.E., Vanhanen J., Lehtipalo K., Gagné S., Neitola K., Mirme A., Mirme S., Tamm E., Uin J., Komsaare K., Attoui M. & Kulmala M. 2009. Results of the first air ion spectrometer calibration and intercomparison workshop. *Atmos. Chem. Phys.* 9: 141–154.

Bellouin N., Jones A., Haywood J. & Christopher S.A. 2008. Updated estimate of aerosol direct radiative forcing from satellite observations and comparison against Hadley Centre climate model. *J. Geophys. Res.* 113, D10205, doi:10.1029/2007JD009385.

Berndt T., Stratmann F., Bräsel S., Heintzenberg J., Laaksonen A. & Kulmala M. 2008. SO_2 oxidation products other than H_2SO_4 as a trigger of new particle formation. Part 1: Laboratory investigations. *Atmos. Chem. Phys.* 8: 6365–6374.

Biskos G., Reavell K. & Collings N. 2005. Electrostatic characterisation of corona-wire aerosol chargers. *Journal of Electrostatics* 63: 69–82.

Cabada J.C., Khlystov A., Wittig A.E. Pilinis C. & Pandis S.N. 2004. Light scattering by fine particles during the Pittsburgh Air Quality Study: measurements and modeling. *J. Geophys. Res.* 109, D16S03, doi:10.1029/2003JD004155.

Dal Maso M., Kulmala M., Riipinen I., Wagner R., Hussein T., Aalto P.P. & Lehtinen K.E.J. 2005. Formation and growth of fresh atmospheric aerosols: eight years of aerosol size distribution data from SMEAR II, Hyytiälä, Finland. *Boreal Env. Res.* 10: 323–336.

Ehn M., Petäjä T., Aufmhoff H., Aalto P., Hämeri K., Arnold F., Laaksonen A. & Kulmala M. 2007. Hygroscopic properties of ultrafine aerosol particles in the boreal forest: diurnal variation, solubility and the influence of sulfuric acid. *Atmos. Chem. Phys.* 7: 211–222.

Fuchs N.A. & Sutugin A.G. 1970. *Highly dispersed aerosols*. Ann Arbor Science Publishers, London.

Flagan R.C. 1998. History of electrical aerosol measurements. *Aerosol Sci. Technol.* 28: 301–380.

Hanson D.R. & Eisele F.L. 2002. Measurement of prenucleation molecular clusters in the NH_3, H_2SO_4, H_2O system. *J. Geophys. Res.* 107, D12, AAC10–1, doi:10.1029/2001JD001100.

Hari P. & Kulmala M. 2005. Station for Measuring Ecosystem–Atmosphere Relations (SMEAR II). *Boreal Env. Res.* 10: 315–322.

Hirsikko A., Laakso L., Hõrrak U., Aalto P.P., Kerminen V.-M. & Kulmala M. 2005. Annual and size dependent variation of growth rates and ion concentrations in boreal forest. *Boreal Env. Res.* 10: 357–369.

Hyslop N.P. 2009. Impaired visibility: the air pollution people see. *Atmos. Environ.* 43: 182–195.

Iida K., Stolzenburg M., McMurry P., Dunn M.J., Smith J.N., Eisele F. & Keady P. 2006. Contribution of ion-induced nucleation to new particle formation: methodology and its application to atmospheric observations in Boulder, Colorado. *J. Geophys. Res.* 111, D23201, doi:10.1029/2006JD007167.

Iida K., Stolzenburg M.R. & McMurry P.H. 2009. Effect of working fluid on sub-2 nm particle detection with a laminar flow ultrafine condensation particle counter. *Aerosol Sci. Technol.* 43: 81–96.

Jokinen V. & Mäkelä J. 1996. Closed loop arrangement with critical orifice for DMA sheath/excess flow system. *J. Aerosol Sci.* 28:643–648.

Kazil J., Harrison R.G. & Lovejoy E.R. 2008. Tropospheric new particle formation and the role of ions. *Space Sci. Rev.* 137: 241–255.

Kerminen V.-M., Lihavainen H., Komppula M., Viisanen Y. & Kulmala M. 2005. Direct observational evidence linking atmospheric aerosol formation and cloud droplet activation. *Geophys. Res. Lett.* 32, L14803, doi:10.1029/2005GL023130.

Knutson E.O. & Whitby K.T. 1975. Aerosol classification by electric mobility: apparatus, theory, and applications. *J. Aerosol Sci.* 6:443–451.

Kuang C., McMurry P.H., McCormick A.V. & Eisele F.L. 2002. Dependence of nucleation rates on sulfuric acid vapor concentration in diverse atmospheric locations. *J. Geophys. Res.* 113, D10209, doi:10.1029/2007JD009253.

Kulmala M. & Tammet H. 2007. Finnish–Estonian air ion and aerosol workshops. *Boreal Env. Res.* 12: 237–245.

Kulmala M. & Kerminen V.-M. 2008. On the growth of atmospheric nanoparticles. *Atmos. Res.* 90: 132–150.

Kulmala M., Pirjola L. & Mäkelä J.M. 2000. Stable sulphate clusters as a source of new atmospheric particles. *Nature* 404: 66–69.

Kulmala M., Lehtinen K.E.J. & Laaksonen A. 2006. Cluster activation theory as an explanation of the linear dependence between formation rate of 3 nm particles and sulphuric acid concentration. *Atmos. Chem. Phys.* 6: 787–793.

Kulmala M., Lehtinen K.E.J., Laakso L., Mordas G. & Hämeri K. 2005. On the existence of neutral atmospheric clusters. *Boreal Env. Res.* 10: 79–87.

Kulmala M., Vehkamäki H., Petäjä T., Dal Maso M., Lauri A., Kerminen V.-M., Birmili W. & McMurry P.H. 2004. Formation and growth rates of ultrafine atmospheric particles: a review of observations. *J. Aerosol Sci.* 35:143–176.

Kulmala M., Hämeri K., Aalto P.P., Mäkelä J.M., Pirjola L., Nilsson E.D., Buzorius G., Rannik Ü., Dal Maso M., Seidl W., Hoffman T., Janson R., Hansson H.-C., Viisanen Y., Laaksonen A. & O'Dowd C.D. 2001. Overview of the international project on biogenic aerosol 20 formation in the boreal forest (BIOFOR). *Tellus* 53B: 324–343.

Kulmala M., Riipinen I., Sipilä M., Manninen H., Petäjä T., Junninen H., Dal Maso M., Mordas G., Mirme A., Vana M., Hirsikko A., Laakso L., Harrison R.M., Hanson I., Leung C., Lehtinen K.E.J. & Kerminen V.-M. 2007a. Towards direct measurement of atmospheric nucleation. *Science* 318: 89–92.

Kulmala M., Mordas G., Petäjä T., Grönholm T., Aalto P.P., Vehkamäki H., Hienola A.I., Herrmann E., Sipilä M., Riipinen I., Manninen H.E., Hämeri K., Stratman

F., Bilde M., Winkler P.M., Wolfram B. & Wagner P.E. 2007b. The condensation particle counter battery (CPCB): a new tool to investigate the activation properties of nanoparticles. *J. Aerosol Sci.* 38: 289–304.

Kulmala M., Asmi A., Lappalainen H.K., Carslaw K.S., Pöschl U., Baltensperger U., Hov Ø., Brenquier J.-L., Pandis S.N., Facchini M.C., Hansson H.-C., Wiedensohler A. & O'Dowd C.D. 2009. Introduction: European Integrated project on Aerosol Cloud Climate and Air Quality interactions (EUCAARI) — integrating aerosol research from nano to global scales. *Atmos. Chem. Phys.* 9: 2825–2841.

Kuwata M., Kondo Y., Miyazaki Y., Komazaki Y., Kim J.H., Yum S.S., Tanimoto H. & Matsueda H. 2008. Cloud condensation nuclei activity at Jeju Island, Korea in spring 2005. *Atmos. Chem. Phys.* 8: 2933–2948.

Laakso L., Mäkelä J.M., Pirjola L. & Kulmala M. 2002. Model studies on ion-induced nucleation in the atmosphere. *J. Geophys. Res.* 107(D20), 4427, doi:10.1029/2002JD002140.

Laakso L., Gagné S., Petäjä T., Hirsikko A., Aalto P., Kulmala M. & Kerminen V.-M. 2007. Detecting charging state of ultra-fine particles: instrumental development and ambient measurements. *Atmos. Chem. Phys.* 7: 1333–1345.

Laaksonen A., Hamed A., Joutsensaari J., Hiltunen L., Cavalli F., Junkermann W., Asmi A., Fuzzi S. & Facchini M.C. 2005. Cloud condensation nucleus production from nucleation events at a highly polluted region. *Geophys. Res. Lett.* 32, L06812, doi:10.1029/2004GL022092.

Laaksonen A., Kulmala M., Berndt T., Stratmann F., Mikkonen S., Ruuskanen A., Lehtinen K.E.J., Dal Maso M., Aalto P., Petäjä T., Riipinen I., Sihto S.-L., Janson R., Arnold F., Hanke M., Ücker J., Umann B., Sellegri K., O'Dowd C.D. & Viisanen Y. 2008. SO_2 oxidation products other than H_2SO_4 as a trigger of new particle formation. Part 2: comparison of ambient and laboratory measurements, and atmospheric implications. *Atmos. Chem. Phys.* 8: 7255–7264.

Lehtipalo K., Sipilä M., Riipinen I., Nieminen T. & Kulmala M. 2008. Analysis of atmospheric neutral and charged molecular clusters in boreal forest using pulse-height CPC. *Atmos. Chem. Phys. Discuss.* 8: 20661–20685.

Lihavainen H., Kerminen V.-M., Komppula M., Hatakka J., Aaltonen V., Kulmala M. & Viisanen Y. 2003. Production of "potential" cloud condensation nuclei associated with atmospheric new-particle formation in northern Finland. *J. Geophys. Res.* 108(D24), 4782, doi:10.1029/2003JD003887.

Lohmann U. & Feichter J. 2005. Global indirect aerosol effects: a review. *Atmos. Chem. Phys.* 5: 715–737.

Lovejoy E.R., Curtius J. & Froyd K.D. 2004. Atmospheric ion-induced nucleation of sulfuric acid and water. *J. Geophys. Res.* 109, D08204, doi: 10.1029/2003JD004460.

Mäkelä J.M., Riihelä M., Ukkonen A., Jokinen V. & Keskinen J. 1996. Comparison of mobility equivalent diameter with Kelvin-Thomson diameter using ion mobility data. *J. Chem. Phys.* 105: 1562–1571.

Makkonen R., Asmi A., Korhonen H., Kokkola H., Järvenoja S., Räisänen P., Lehtinen K.E.J., Laaksonen A., Kerminen V.-M., Järvinen H., Lohmann U., Bennartz R., Feichter J. & Kulmala M. 2009. Sensitivity of aerosol concentrations and cloud properties to nucleation and secondary organic distribution in ECHAM5-HAM global circulation model. *Atmos. Chem. Phys.* 9: 1747–1766.

Marti J.J., Weber R.J., Saros M.T., Vasilou J.G. & McMurry P.H. 1996. Modification of the TSI 3025 condensation particle counter for pulse height analysis. *Aerosol Sci. Technol.* 25: 214–218.

McMurry P.H. 2000a. A review of atmospheric aerosol measurements. *Atmos. Environ.* 34: 1959–1999.

McMurry P.H. 2000b. The history of CPCs. *Aerosol Sci. Technol.* 33: 297–322.

Mirme A., Tamm A., Mordas G., Vana M., Uin J., Mirme S., Bernotas T., Laakso L., Hirsikko A. & Kulmala M. 2007. A wide-range multi-channel air ion spectrometer. *Boreal Env. Res.* 12: 247–264.

O'Dowd C., McFiggans G., Creasey D.J., Pirjola L., Hoell C., Smith M.H., Allan B.J., Plane J.M.C., Heard D.E., Lee J.D., Pilling M.J. & Kulmala M. 1999. On the photochemical production of new particles in the coastal boundary layer. *Geophys. Res. Lett.* 26: 1707–1710.

Pierce J.R. & Adams P.J. 2009. Uncertainty in global CCN concentrations from uncertain aerosol nucleation and primary emission rates. *Atmos. Chem. Phys.* 9: 1339–1356.

Riipinen I., Sihto S.-L., Kulmala M., Arnold F., Dal Maso M., Birmili W., Saarnio K., Teinilä K., Kerminen V.-M., Laaksonen A. & Lehtinen K.E.J. 2007. Connections between atmospheric sulphuric acid and new particle formation during QUEST III–IV campaigns in Hyytiälä and Heidelberg. *Atmos. Chem. Phys.* 7: 1899–1914.

Riipinen A., Manninen H.E., Yli-Juuti T., Boy M., Sipilä M., Ehn M., Junninen H., Petäjä T. & Kulmala M. 2009. Applying the Condensation Particle Counter Battery (CPCB) to study the water-affinity of freshly-formed 2–9 nm particles in boreal forest. *Atmos. Chem. Phys.* 9: 3317–3330.

Sihto S.-L., Kulmala M., Kerminen V.-M., Dal Maso M., Petäjä T., Riipinen I., Korhonen H., Arnold F., Janson R., Boy M., Laaksonen A. & Lehtinen K.E.J. 2006. Atmospheric sulphuric acid and aerosol formation: implications from atmospheric measurements for nucleation and early growth mechanisms. *Atmos. Chem. Phys.* 6: 4079–4091.

Sipilä M., Lehtipalo K., Kulmala M., Petäjä T., Junninen H., Aalto P.P., Manninen H.E., Kyrö E.-M., Asmi E., Riipinen I., Curtius J., Kürten A., Borrmann S. & O'Dowd C.D. 2008. Applicability of condensation particle counters to measure atmospheric clusters. *Atmos. Chem. Phys.* 8: 4049–4060.

Sipilä M., Lehtipalo K., Attoui M., Neitola K., Petäjä T., Aalto P.P., O'Dowd C.D. & Kulmala M. 2009. Laboratory verification of PH-CPC's ability to monitor atmospheric sub-3 nm clusters. *Aerosol Sci. Technol.* 43: 126–135.

Spracklen D.V., Carslaw K.S., Kulmala M., Kerminen V.-M., Sihto S.-L., Riipinen I., Merikanto J., Mann G.W., Chipperfield M.P., Wiedensohler A., Birmili W. & Lihavainen H. 2008. Contribution of particle formation to global cloud condensation nuclei concentrations. *Geophys. Res.*

Lett. 35, L06808, doi:10.1029/2007GL033038.

Tammet H. 2006. Continuous scanning of the mobility and size distribution of charged clusters and nanometer particles in atmospheric air and the Balanced Scanning Mobility Analyzer BSMA. *Atmos*. *Res*. 82: 523–535.

Wang M. & Penner J.E. 2009. Aerosol indirect forcing in a global model with particle nucleation. *Atmos*. *Chem*. *Phys*. 9: 239–260.

Weber R.J., Marti J.J., McMurry P.H., Eisele F.L., Tanner D.J & Jefferson A. 1996. Measured atmospheric new particle formation rates: implications for nucleation mechanisms. *Chem*. *Eng*. *Comm*. 151: 53–64.

Weber R.J., Marti J.J., McMurry P.H., Eisele F.L., Tanner D.J. & Jefferson A. 1997. Measurements of new particle formation and ultrafine particle growth rates at a clean continental site. *J*. *Geophys*. *Res*. 102: 4375–4385.

Vehkamäki H., Kulmala M., Napari I., Lehtinen K.E.J., Timmreck C., Noppel M. & Laaksonen A. 2002. An improved parameterization for sulfuric acid-water nucleation rates for tropospheric and stratospheric conditions. *J*. *Geophys*. *Res*. 107(D22), 4622, doi:10.1029/2002JD002184.

Winkler P.M., Steiner G., Virtala A., Vehkamäki H., Noppel M., Lehtinen K.E.J., Reischl G.P., Wagner P.E. & Kulmala M. 2008. Heterogeneous nucleation experiments bridging the scale from molecular ion clusters to nanoparticles. *Science* 319: 1374–1377.

Yu F. & Turco R. 2008. Case studies of particle formation events observed in boreal forests: implications for nucleation mechanisms. *Atmos*. *Chem*. *Phys*. 8: 6085–6102.

Yu F., Wang, Z., Luo G. & Turco R. 2008. Ion-mediated nucleation as an important global source of tropospheric aerosols. *Atmos*. *Chem*. *Phys*. 8: 2537–2554.